https://ntrs.nasa.gov/search.jsp?R=19690006587 2020-03-12T08:19:46+00:00Z

General Disclaimer

One or more of the Following Statements may affect this Document

- This document has been reproduced from the best copy furnished by the organizational source. It is being released in the interest of making available as much information as possible.
- This document may contain data, which exceeds the sheet parameters. It was furnished in this condition by the organizational source and is the best copy available.
- This document may contain tone-on-tone or color graphs, charts and/or pictures, which have been reproduced in black and white.
- This document is paginated as submitted by the original source.
- Portions of this document are not fully legible due to the historical nature of some of the material. However, it is the best reproduction available from the original submission.

Produced by the NASA Center for Aerospace Information (CASI)

THE APPLICATION OF THE SCANNING ELECTRON MICROSCOPE TO STUDIES OF CURRENT MULTIPLICATION, AVALANCHE BREAKDOWN AND THERMAL RUNAWAY

(II) - General studies, mainly non-thermal

by

D. V. Sulway, R. C. Wayte and P. R. Thornton

School of Engineering Science
U. C. N. W., Dean Street,
Bangor, Caerns., U. K.

University College of North Wales

NGR-52-117-001

N 69-15919
(ACCESSION NUMBER) (THRU) 1
47 (PAGES) (CODE) 23
CR 99041 (NASA CR OR TMX OR AD NUMBER) (CATEGORY)
FACILITY FORM 602

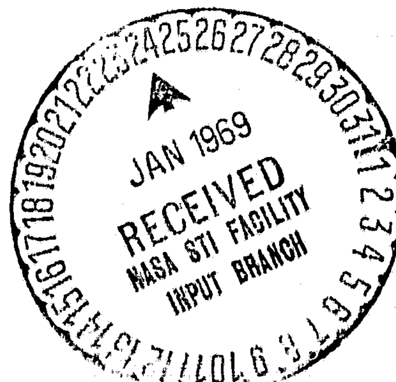

The application of the scanning electron microscope to studies of current multiplication, avalanche breakdown and thermal runaway (II) - General studies, mainly non-thermal.

I. Introduction

In recent years a wealth of information about the microscopic aspects of avalanche effects has become available mainly as a result of the work of the Clevite group ((1), (2), (3) and (4)). At the same time considerable theoretical work has been done, in particular of the way in which 'hot spots' can develop and lead to thermal runaway (5). Most of the experimental work has relied on the use of refined travelling light spots to obtain information about current multiplication. This technique is limited in spatial resolution and can be time consuming, even in its most recent form (6) which employs a laser. The scanning electron microscope can be used as an ultra refined travelling source of electron-hole pairs, in which the scanning is easily controlled or automated, the resolution is high, the depth of penetration can be varied and the excitation level varied by six orders of magnitude. Before this approach can be generally exploited it is necessary to establish the relative importance in practice of the various contrast mechanisms that can be imagined.

As a suitable approach to examine these mechanisms we selected a practical problem presented to us by a microcircuit manufacturer. It had been found that some Read diodes intended for use as microwave oscillators contained sources of excess noise and it was of interest to isolate the cause of this detrimental effect. This structure was therefore used also as a 'vehicle' for the more fundamental studies.

The experimental methods used are conventional and have been described fully elsewhere (7) but, in brief, consist of using the charge collection current induced in a pn junction by a scanning electron beam to control the brightness of a CRT which is scanned in synchronism with the primary beam. In this way 'maps' of the charge collection signal can be obtained. Physically the method is analogous to the travelling light spot technique or to the processes involved in the detection of γ rays, for example, by solid state particle counters (8). In the present work the signal was exploited in two other ways; (a) with the primary beam constrained to move along a prechosen line the signal is fed to the Y plates of a CRT or

of an XY recorder the X deflection of which is controlled by the time base moving the primary beam. In this way the variation of the signal along the line is recorded, (b) with the primary beam kept stationary at a prechosen spot the bias on the diode is 'ramped' up to a maximum value and down again and the beam induced signal recorded as a function of time, i.e. diode bias. Where relevant, the surface of the device was examined by using the SEM to obtain a micrograph of the surface by using secondary electron emission. These surface micrographs we shall call 'emissive' micrographs in contrast to the 'conductive' micrographs used to study the underlying junctions. Other special techniques are described in the relevant sections.

Finally, it should be stressed that we have limited the discussion of these initial results to effects which are mainly non-thermal in origin. A clear-cut division is not possible because of the interactions between non-thermal and thermal processes. The mainly thermal effects will be discussed in a further paper.

2. General results

Figure 1(a) shows a schematic cross section through the Read diodes used. The size of the active area is, in fact, about 100 μ x 100 μ. The Al contacts were 1,000Å thick and the oxide thickness was 1μ. Figure 1(b) illustrates the cause of the

rejection of these devices. The top right hand current voltage characteristic shows the typical discontinuities observed in the VI curves just after breakdown. The left hand curve shows a magnified view of the knee of the curve. Finally, figure 1(b) shows the curve obtained after the device had been damaged by thermal runaway and is relevant to the later discussion. Examination of the surface (figure 3(c) and at higher magnification) revealed no details of significance, but examination of the charge-collection maps revealed the presence of arrays of dislocations having a three fold symmetry. See figure 1(d). As the bias was increased local breakdown occurred at various sites on this dislocation array. The occurrence of these microplasmas suggested that they are not an intrinsic property of the dislocations themselves but are associated with some secondary fault associated with the dislocations. The sequence of micrographs shown illustrate the behaviour of the localised breakdown as a function of bias. We were able to relate these regions of localised breakdown to the discontinuities on the VI curve and to the noise properties. These observations therefore relate the fault to a mechanical defect and suggests a means of

eliminating it by removing the mechanical defect. We shall discuss the physical origin of the mechanical defect in more detail below after reporting further observations of the device after it had been ion-etched.

3. Initial observations of microplasma behaviour

3(a) Interactions between microplasmas

In figure 1(h) there are two main microplasmas in the lower half of the figure and a third is just evident in the top left hand corner. Subsequent increase in bias leads to an increase in signal from this third microplasma while at the same time the signals from the lower two decrease (see figure I(i)), because the voltage corresponding to the peak signal in these regions has been exceeded. However, still further increase in applied bias results in a very big signal from the top left hand corner microplasma and the current flowing through this region appears to affect the voltage distribution at the other two. We can explain the sudden increase in signal (see figure I(j)) from the two lower regions if we assume that the current flow at the upper regions lowers the voltage drop across the lower regions. This interaction behaviour has to be taken into account when interpreting the results of voltage ramp studies from a fixed location.

3(b) Thermal effects associated with microplasmas

Further increase in device bias leads to changes in contrast which appear to be related to thermal effects. Consider figure I(k), for example. The contrast at the microplasmas changes to the circular regions shown in more detail in figures I(l) and (m) at higher magnification. In addition there is a general loss of signal from the bulk of the active area. These changes do not occur immediately after the application of a bias increment, but, depending on the magnitude of voltage increment, take seconds or tens of seconds. These effects are reversible and can be repeated as the voltage is cycled. However, if the bias is further increased, the 'black' region in the centre of the active area increases in 'blackness' and extent. When it reaches the region of the lower left hand microplasma the device 'runaway' and the VI curve becomes degraded to the extent shown in figure I(b). The appearance of the device after damage is shown in figure I(o) (a conductive map) and in figure I(p) (an emissive micrograph of the surface immediately after damage). It is apparent that a highly conductive channel has developed across the junction and that this channel involves both the site of the lower left hand micro-plasma and the top contact. The nature of the damage was revealed in more detail by ion-etching.

3(c) Results obtained by ion etching

The observations of the damage regions are obscured by the surface 'debris' left as a result of the thermal runaway. In order to examine the damage regions in more detail the 'debris' and the surface layer was removed by ion etching. The method used is a slightly more controlled version by the method pioneered by Stewart (9) and later by Broers (10). The ions used were argon ions accelerated to 5kV. A current of the order of 10^{-5} amps was focussed into a preselected area of the order of 1 mm. The etching time was approximately 30 minutes. Figure 2 shows the results obtained. Figures 2(a) to (d) are surface micrographs of the device studied in figure 1. A second device was used to obtain the micrographs in figures 2(e) and (f). It is apparent that, in each case, the damaged region consists of a 'furrow' with material 'heaped up' at the furrow edge. The furrow connects the localised region where the thermal runaway began with the metal bond. In each case the runaway began where a dislocation or dislocation group was situated. This is shown particularly clearly in figures 2(c) and (f). The runaway occurred when the dark region of low signal interacts

with the microplasmas inherent at the dislocation regions i.e. when the dark region (see figure 1(n)) reaches the microplasma region. We believe that the darkened region is associated with a temperature rise associated with Joule heating.

Another observation of importance can be seen in micrographs 2(a) and (d) in which the diode studied had been relatively deeply etched. This observation concerns the fact that ion-etched etch-pits are observed well outside the active p+ region.

This observation is relevant to the question of the origin of the dislocations causing the microplasmas and the associated noise. This question is discussed in the next section.

4. Initial discussion

These results provide information about the origin of the dislocations responsible for the excess noise observed, some features of microplasma behaviour and about possible causes of thermal runaway. We now consider each in turn.

There are two possibilities for the origin of the observed dislocations. One is that the dislocations are related to the tetrahedral arrays of stacking faults observed in epitaxially deposited

material grown on poorly prepared substrates (11). The other possibility is that the dislocations are arrays induced by heavy doping during diffusion. The probability is that the dislocations are stacking faults. The evidence in support of this idea is that (1) the ion etching studies (see figure 2) show that the dislocations occur well outside the diffused areas and (2) the doping level used in the p+ region is $\sim 3 \times 10^{18}$ cm^{3} which is too low for the formation of diffusion induced dislocations. Attempts to confirm these observations by measuring the size of the triangular defects and correlating this to the known thickness of the epitaxial layer were unsuccessful because of the variation in size of the triangular defects.

At high diode currents the contrast observed at the 'core' or centres of the predominant microplasmas changes into circular patterns which apparently vary in character from one microplasma to another. See figures 1 (o) and (n). The degree of the circular symmetry of this high current contrast is striking. It is reversible and appears to be related to thermal effects. As it is possible that this contrast could reveal information about localised defects and the way in which they contribute to thermal runaway it is important

to investigate the way in which this contrast depends on the physical parameters of importance to localised breakdown.

The onset of permanent damage appears to be associated in this case with an interaction between bulk Joule heating and the core of the microplasma. But, before this idea can be substantiated it is necessary to confirm that the region of dark signal seen in figures 1(k) and (n) for example, are in fact, due to an increase in temperature.

To provide further evidence on these and other points the more detailed observations on microplasma behaviour described in the next section were made.

5. More detailed studies of microplasma behaviour

5(a) Behaviour at low currents

The complexity of the observed behaviour at high currents meant that we had to study the behaviour at low currents i. e. at currents below those at which bulk thermal effects occur. Only by first understanding results in this regime can we hope to understand the importance of thermal effects and to apply the method to thermal runaway studies. Figure 3 shows more detailed studies of one of the Read diodes used in this work. In this sequence the

diode bias and the beam voltage were kept constant and only the beam current varied in the manner indicated in the caption. The system gain was varied to keep the output signal within the working range of the film. The bias voltage chosen was just beyond the knee in the VI curve. There are two interesting observations in this sequence, one is that the contrast behaviour from one localised region is dependent on the excitation level used. This is very apparent for the main microplasma (marked A in figure 3), for the subsidiary row of defects (B in figure 3) associated with the dislocation network and for the smaller microplasma(marked C in figure 3.) The second interesting observation is that the relative signals from different areas also vary with the excitation level used. This variation means that it is necessary to do very careful studies indeed if we seek to examine the extent of microplasma regions in depth by varying the beam voltage. Because, not only does the mean depth of penetration vary as the beam voltage is changed, but the excitation level changes as well. As a result a depth dependence of signal occurs in conjunction with an excitation dependence.

5(b) Quantitative observations (i) line scans

Figure 3 does not indicate the full magnitude of this excitation

dependence. To obtain this information the line scans shown in figures 4 and 5 were obtained along a line through the microplasma A and the line of defects marked B in figure 3. In order to relate the given curves to the VI characteristic we have included the current voltage characteristic in figure 6. The main features of these observations can be summed up as follows:-

(1) At low excitation levels (i.e. $I_b = 3 \pm 1 \times 10^{-13}$ amps at 15 kV) each regions acts independently of the surrounding regions. Very high values of current multiplication were obtained from regions where defects had caused an enhancement of the field (at microplasmas). Under these conditions all the inherent variations in current multiplication are observed, each region giving an increasing signal at first as the bias is increased and then a rapidly decreasing output as the bias is further increased.

(2) As the excitation level is increased somewhat the height of the major multiplication peaks decreases compared to the signal from the bulk of the active area. At the same time the effective area of the major peaks extends. As a result some of the peaks merge and some of the variations observed at lower beam currents are not observed.

(3) As the excitation level is increased further the signal behaviour from the centre or 'core' of the more predominant micro-plasma changes in character. The main changes are shown schematically in figure 7. At low beam currents the line scan across the major defect consists of a single peak which increases in height as the bias is increased, but varies little in shape and extent except at very high biases where a small 'dip' occurs at the centre. See figure 7(a). At somewhat higher beam currents the 'core' signal develops further structure. As the diode bias is increased the 'dip' first develops in the centre and then a subsidiary 'halo' develops around the central minimum. See figure 7(b). Subsequent increase in bias voltage results in an increase in the depth of the central minimum so that the halo ultimately disappears. At higher beam currents this sequence is repeated more rapidly as the bias is increased so that at the higher bias levels the core signal appears as a deep minimum surrounded by a bright annular peak signal.

(4) At the highest beam current levels the signal from the main microplasma is diminished so that it is equal or less than the signal from the bulk area. Under these conditions the core signal from the main microplasma consists of central peak surrounded by a halo of reduced signal. See figures 5 and 7(e).

In general these measurements were discontinued at biases before the device became unstable due to excessive Joule heating. The maximum variation experienced due to Joule heating is shown by the shaded area in figure 5(b). Usually the graphs shown are reliable to within 2 to 3 times the width of the line in the drawing. This reliability was checked periodically by repeating certain of the line scans.

5(c) Quantitative observations (2) stationary beam studies

To complete the information about the excitation dependence we used a stationary electron beam and obtained the charge collection signal as the bias voltage was ramped through the voltage corresponding to the peak signal. The values of the peak signals obtained at two beam voltages are shown in figure 8. The behaviour is very variable depending on the site chosen. Consider a site in the centre of the main microplasma. With a beam voltage of 15kV the peak signal is approximately constant independent of the beam current used except at the higher beam currents, where there is a slow increase in signal with increase in current. By way of contrast the signal from a bulk region remote from any microplasma increases proportionately with the beam current. The behaviour from a

smaller microplasma lies intermediate between these two extremes. At a beam voltage of 5kV, the signal from the main microplasma is again constant, independent of beam current, whereas both the bulk signal and the signal from the other microplasma studied increase roughly as I_b^{α} with $.5 < \alpha < .7$.

Data derived from figure 8 and other studies are shown in figure 9 where the effective maximum multiplication is plotted for each of the regions studied. To a first order approximation the values obtained from the large microplasma vary according to the equation M_{eff} x beam watts = constant where the constant increases with decrease in beam voltage. This expression is reasonably well obeyed at all beam voltages except at very low beam voltages and very low beam currents where there is some evidence that the very high values of the multiplication obtained lead to a saturation effect. The bulk region shows the inverse relationship only at high wattage. At lower wattages the effective multiplication increases only slowly with decrease in wattage although there is some indication that, at the lowest wattages, M begins to increase rapidly again. For the bulk region this behaviour is observed at both 5 and 15kV.

By way of contrast the behaviour of the small microplasma is sensitive to changes in beam voltage. At 15kV the behaviour of this region follows that of the large microplasma whereas at 5kV the behaviour is that characteristic of the bulk region.

5(d) Temperature measurements by infra-red microscopy

We used an infra red microscope to confirm that localised heating occurred at microplasmas. The IR microscope was used in a conventional way to measure the total radiance from a selected area. The devices used were studied after a thin layerof carbon had been evaporated onto the surface to increase the surface emissivity. Only approximate estimates of the absolute temperature can be obtained as the emissivity is known only approximately and was taken as 0.9. The experimental procedure adopted was to use the SEM to locate the microplasmas in a given device and to determine the voltage at which the microplasmas turn on. Subsequently, the temperature distribution around the microplasmas was measured with the bias kept constant at a value such that the main microplasmas were 'on' but such that the bulk Joule heating was not sufficient to damage the device or cause instabilities. The results are typified by noting that, with a room

temperature of $24\frac{1}{2}^{o}$C and a bulk junction temperature of 30°C the temperatures of two microplasma cores on one device were 40°C and 50°C. Bearing in mind that these measurements were taken with an optical system which integrates over 10 microns these estimates of the local temperature enhancement must be regarded as lower limits to the true peak values.

6. Interpretation

6(a) General background

It is generally assumed that the processes occurring at microplasmas are basically the same as those occurring in bulk breakdown except that they differ in degree because of localised variations in field strength etc. To date it has been a satisfactory approximation to regard an avalanching element of the device as a current source with three components to the series resistance associated with it:-

(a) The spreading resistance. This component arises because of the small diameter, D, of the element and can be written as $R_{sp} = \rho/2D$ where ρ is the resistivity of the bulk regions.

(b) The space charge resistance. This component arises because the high field in the avalanching region separates the electrons and holes and so creates a dipole field which opposes the applied field. The

equivalent resistance can be written (12) R_{sc} $W^2/2qV_dA$, where W is the width of the junction, V_d is the limiting drift velocity and A is the area of the element considered.

(c) The thermal 'resistance'. This contribution has its origin in the temperature dependence of the breakdown voltage i. e. as an element heats up its breakdown voltage increases and so its current carrying ability under constant bias decreases, i. e. its resistance increases.

For completeness a shunt resistor, R_s, should be included in the circuit in the present context to take account of the fact that some of the electron beam induced excitation can be neutralised by internal processes and so does not contribute to the current in the external circuit. For the present we shall neglect this shunt resistor and collect the various series contributions together to give a total series resistance R'_L which, if the element considered is the whole diode, can be related to the slope resistance of the diode. This series resistance determines the shape of the multiplication against voltage curve. Initially as the voltage is increased, the field and, therefore, the current multiplication increases. But once the diode element begins to pass a significant dark current another situation develops. Firstly, a finite voltage drop develops across the series resistance which tends to limit the field that can be

applied to the avalanching region and so limits the multiplication of the beam induced carriers. In addition, at voltages above breakdown the number of dark carriers reaching a given element increases because of multiplication in the surrounding elements etc. As a result the photocarriers have to compete with the dark current, or, to put it another way, an increasing proportion of the photocarriers arrive when the element is avalanching and so cannot be multiplied. Therefore the effective multiplication drops. In addition, when the applied bias is increased beyond a given value under certain conditions of excitation the increment of voltage appearing across the series resistor is greater than the increment in the applied voltage. As a result the voltage across the avalanche region drops and the multiplication falls (13). As a result of these effects the multiplication curve as a function of voltage takes the form shown in figure 10(a). This figure also shows the way in which temperature effects the curve. In brief an increase in temperature increases the value of the voltage at which the peak occurs, the peak value is lowered a little and the breadth of the peak increases marginally (14).

These observations can be used to explain the experimental data described in section 5.

6(b) Interpretation of the contrast effects observed at a microplasma core.

It is most convenient to consider first the relatively complex effects at moderate excitation levels. We have already outlined in section 5(a) how the signal from a given element varies as the bias is varied. This variation is shown in figure 10(a) together with the way in which the curve varies with temperature. We can use these facts to interpret the observed contrast. Consider the idealised situation shown in figure 10(b) where the local breakdown voltage varies linearly with distance. With the applied voltage set at the value shown in figure 10(b) the signal will vary in the manner shown in figure 10(c). The numbers shown in figure 10(b) correspond to those in figure 10(a). The above description is adequate provided there is no temperature variation across the core. Let us consider the case where the temperature increases monotonically towards the core centre. If this is the case the local breakdown voltage curve will follow one of the forms shown in figure 10(d) depending on the local temperature distribution. With this kind of distribution the multiplication signal will take one of the forms shown in figure 10(e).

This model, which relies on the variation of V_b with junction thickness and the variation of V_b with temperature (the thermal resistance discussed in the literature and in section 6(a)), can explain the sequences shown in figure 7(b), (c) and (d). However, further explanation is necessary of the excitation dependence of this effect in particular it is necessary to explain why these relative complex patterns are observed only over a given range of excitations and not at low excitations except at high bias and not at all at high excitations.

At high excitations the observed contrast probably arises because there is a thermal interaction between the surrounding elements which are passing a large current as well as the microplasma core. In this case the 'bulk' Joule heating may be enhanced locally by the local heating in the microplasma core. The envisaged situation is shown in figures 10(f) and (g) where the combined thermal resistance and the built in field variation produce the variation of V_b shown in figure 10(g). With the applied bias set at the value shown in this figure the charge collection signal will vary in the manner shown in figure 10(h). This situation explains the situations shown at high biasses in figure 7(e). It is also consistent with the observations of the manner in which thermal runaway occurs. (See section 3(b)).

The relative absence of these effects at low excitation may, at first sight, be related to the possibility that the beam itself causes some heating. With a 20kV beam and current levels of between 10^{-13} and 10^{-17} amps remaining on the microplasma for a time τ between $2 \times 10^{-9}\tau$ to $2 \times 10^{13}\tau$ watts are delivered by the beam to the core. This figure has to be compared with some 10^{-3} watts resulting from the dark current flow (e.g. at microplasma carrying 10 [illegible] a at 100V). Therefore with a scanning beam this 'beam heating' is likely to be of minimal importance. Therefore we still have to explain the behaviour at low excitations. At present we have no clear indication of the additional factor which has to be incorporated into the model to explain this dependence.

6(c) Interpretation of peak values of M_{eff}

The basic idea that is exploited here is that each incoming carrier has a finite chance of causing a burst of multiplication. This probability decreases as the fraction of the time the microplasma is 'on' increases. As a result the beam induced multiplication reaches a limiting i. e. peak value. The multiplication is defined by

$$M_{eff}(V) = I(V) / I(0) = I_1 \phi_1 / qN_o \qquad \text{......... eq. 1}$$

where l_1 is the current carried by the microplasma in the fully 'on' condition, ϕ_1 is the fraction of time the microplasma is 'on' and N_o is the number of beam induced electrons reaching the area per second. The peak value will occur when $\phi_1 = 1$ so that

$$M_{peak} \quad l_1 / qN_o \quad E_i l_1 / qV_p I_p f(V_p) \ldots\ldots \text{ eq. 2}$$

where E_i is the ionization energy, V_p is the beam voltage, I_p is the primary beam and $f(V_p)$ is the fraction collected by the microplasma region. Equation 2 explains some of the observations shown in figure 9. Consider the main microplasma. In general terms M_{peak} is proportional to $(V_p I_p)^{-1}$ in accord with equation 2. The dependence on $f(V_p)$ is also as predicted at 15kV and 5kV in that $f(V_p)$ appears to be independent of I_p as is normally assumed. In addition $f(V_p)$ decreases as V_p is decreased in accord with the assumption that the microplasma 'core' is relatively deep i. e. of the order of the penetration distance of a 15kV beam or greater. However, the results at 3kV seem to require an additional assumption to fit the observations. The fact that M_{peak} falls off less rapidly than $(V_p I_p)^{-1}$ at low excitation levels could be interpreted on the idea that, at 3kV, $f(V_p)$ is a function of I_p. The apparent dependence required is that $f(V_p)$ varies as $I_p^{-\alpha}$ where $\frac{1}{3} < \alpha < \frac{1}{2}$

It is possible that this departure from the usual behaviour is due to the presence of fast surface states at the silicon surface. In the present context these fast states can act as an additional sink for free carriers and so compete with the junction charge collection process. This effect will only be important for low beam energies. It would also be excitation dependent in that the fraction of the beam induced carriers lost to the charge collection process through surface recombination will vary with the density of carriers injected compared to the density of suitable surface states. The best way in which this possibility can be studied is by using a structure in which the surface voltage canbe varied by means of a gate contact.

The behaviour of the bulk region is different in that the increase in M_{peak} with decrease in excitation level is not maintained at low levels. In terms of equation 2 this result implies that either I_1 or $f(V_p)$ is dependent on the excitation current. It is unlikely that $f(V_p)$ is dependent on I_p as there is no evidence known to the authors indicating that such a dependence has been observed or has been suggested in explanation of other data. It is of interest to consider whether I_1 can vary with I_p. In this context it must be remembered that the elements surrounding the point examined are avalanching at the same time, in

contrast to the situation at a microplasma which is, in essence, an isolated avalanching region in a non avalanching background. It is possible that an interaction between the bulk elements could lead to a variation of l_1 with excitation if the degree of interaction is dependent on excitation level. If, at high excitation levels, beam induced carriers can, in effect, diffuse into adjacent area and cause multiplication l_1 would increase with current. Finally, if this effect saturated at high currents the form of the M_{peak} against wattage curve could take the form shown in figure 9.

It is obvious that if we impose a coupling mechanism between the avalanching elements and stipulate that the coupling efficiency can vary from site to site we can obtain a whole variety of behaviour between the two extremes shown in figure 9. The behaviour of the small microplasma is thus explicable except in one aspect. The question remains as to why, on this model, the coupling mechanism varies in efficiency as the depth of the beam varies. At 15kV the coupling mechanism appears to be relatively ineffective compared to a 5kV beam. At first sight this is an unexpected result as it seems more probable that a beam with deeper pentration would lead to more

effective coupling. In the absence of other indications the behaviour of the small microplasma would lead us to query the importance of the coupling process. but we know from voltage 'ramp' studies that a coupling mechanism is probably operative because two or more peaks in the multiplication against bias voltage curve and a simple explanation can be obtained in terms of a coupling mechanism (14). We also know from Haitz's work that an optical coupling mechanism can operate over distances of up to 1.8 mm. (4). It is also possible that inter actions can occur because current flow through one region can effect the voltage distribution at another. In view of these supporting indications it is apparent that more work is required to establish the validity of this idea and the way in which the details vary from region to region. These studies are best made in connection with voltage ramp studies of thermal effects.

7. Summary and conclusions

The main conclusions can be summarised by the following list:-

(1) The excess noise in the Read diodes studied is associated with a dislocation network existing in the diodes.

(2) The noise is not an intrinsic property of the dislocation network but is caused by microplasmas associated with the network.

(3) The exact origin of the microplasmas is not known but it is likely that a second phase associated with the dislocation array is causing localised field enhancement.

(4) The cause of the dislocations is not definitely known, but the concensus of the evidence is that the array is due to insufficient care in substrate preparation with the result that tetrahedral arrays of stacking faults are nucleated at the interface between substrate and epitaxial growth.

(5) The contrast features of the microplasma 'cores' are complex but in the main can be interpreted in terms of a localised field enhancement together with localised heating.

(6) The presence of the localised heating at the microplasma 'core' has been confirmed by infra red microscopy.

(7) The variation of breakdown voltage with temperature can be used to obtain information about the bulk temperature distribution in the device. Although further work is needed to establish the worth of the method it has already shown that the onset of thermal runaway in these devices occurs when the bulk Joule heating interacts with the localised heating at a microplasma 'core' to cause an unstable hot spot.

(8) Measurements of peak multiplication have been made over a far wider range of excitation levels than has been hitherto possible.

The behaviour, both in the bulk and at microplasma 'cores', can be complex and suggests that the currently accepted model of avalanche behaviour may need modification in detail by introducing an excitation dependence of some of the parameters usually assumed to be independent of excitation level. The origin of this excitation dependence is not known but may be related to coupling between avalanching 'cells'.

(9) This complexity of the excitation dependence makes it difficult, not only to give a unique interpretation to the observed contrast, but complicates the examination of hot spots in depth. Because, as the beam penetration is increased, not only does the thickness of the layer examined increase but also the excitation level in the upper parts of the layer changes. Therefore the changes in relative signal from the various parts of a hot spot which occur when the penetration is varied can be due to both causes. From this compounded signal we have to seek to establish the multiplication as a function of depth at a constant excitation. Because of this interpretative problem we are establishing a second approach in parallel, in which the SEM is used to locate the microplasmas, the devices are

then sectioned at right angles to the junction to bring the micro-plasma cores within about 10μ of the sectioned surface and then to examine the core 'sideways on' rather than in depth. This method replaces interpretative difficulties by experimental problems. With this combination of methods the best chance of examining the details of localised breakdown is achieved.

Captions to Figures

Figure 1 (a) line diagram showing the cross section of the devices studied, (b) VI characteristics of the device before and after damage by thermal runaway. (c) Emissive micrograph of the device surface; (d) conductive micrograph of the device taken at zero volts bias. (e) to (k) conductive micrographs taken at 64.5, 100.4, 104.7, 108.8, 111.3, 115.1, and 118.1 volts respectively, (l) and (m) are magnified views of parts of (k); (n) conductive micrograph taken at 119 volts, (o) conductive micrograph taken after the device had been damaged and (p) the corresponding emissive micrograph of the damaged device.

Figure 2 Ion etching studies of damaged devices. (a) General view of a damaged device, after ion etching, (b), (c) and (d) magnified views of part of the diode shown in (a); (e) and (f) emissive micrographs of the device studied in figure 1 after ion etching.

Figure 3 Conductive micrographs of another Read diode showing how the observed contrast is excitation level dependent.

Figure 4 Line scans taken along the line through the microplasma marked A and the line of defects marked B in figure 3. The sequence marked (a) was obtained with a . 15kV beam carrying 3×10^{-13} amps whereas (b) was obtained with 3×10^{-12} amps at the same kV.

Figure 5 Continuation of the data shown in figure 4(c) excitation current = 2.0×10^{-9} amps; (d) excitation current = 2.0×10^{-8} amps.

Figure 6 The current voltage characteristic for the diode studied in figures 3, 4 and 5.

Figure 7 Schematic drawings showing the main changes in contrast at a microplasma 'core' as the diode bias and excitation current is varied. (a) With low excitation currents, (b) with slightly higher beam currents under the lower diode bias conditions; (c) continuation of (b) at increasingly high bias (d) and (e) repeats of the previous behaviour at high and very high beam currents.

Figure 8 Plots of the peak charge signal against beam current for 3 regions. The main microplasma is that marked A in figure 3, the small microplasma is that marked C and the bulk region is the 'dark' region near the edge of the device above the main microplasma in figure 3. (a) Taken at a beam voltage of 15kV, (b) taken at 5kV.

Figure 9 Values of the peak multiplication obtained from the data in figure 8 and from further measurements.

Figure 10 (a) Idealised curves of M against bias as a function of temperature, T_2 T_1; (b) postulated distribution of breakdown voltage, V_b, at a microplasma core in the absence of heating relative to the applied voltage, V_a; (c) the charge collection signal corresponding to the situation shown in (b); (d) corresponding to (b) but .owing for various degrees of local heating; (e) the charge collection signals corresponding to the various cases shown in (d); (f) components to overall variation of V_b, $V_b(T)$ = variation due to temperature change,

V_b (z) = built-in variation; (g) total variation of V_b as a function of position relative to applied voltage; (h) charge collection signal corresponding to (g).

References

(1) A. Goetzberger and W. Shockley, J. Appl. Phys., 31, 1821, (1960).

(2) A. Goetzberger, Bull. Amer. Phys. Soc., 5, 160, (1960).

(3) W. Shockley, Solid State Electron., 2, 1, (1961).

(4) R.H. Haitz, Solid State Electron., 8, 417, (1965).

(5) A.C. English, I.E.E.E. Trans. Elec. Dev., ED-13, 8-9, (1966).

(6) G. Dalmann, paper presented at the Second Manchester Conference on Solid State Devices, (September, 1968).

(7) See P.R. Thornton, Scanning Electron Microscopy, Chapman and Hall, (1968).

(8) G. Dearnaley and D.C. Northrop, Semiconductor Counters for Nuclear Radiations, E. and F.N. Spon Ltd. (1963).

(9) A.D.G. Stewart, Proc. 5th Inter. Conf. on Electron Microscopy, Philadelphia, (ed. S.S. Breese), Academic Press, New York (1962).

(10) A.N. Broers, Ph.D. Thesis, Cambridge (1965).

(11) H.J. Quiesser and A. Goetzberger, Phil. Mag., 8, 1063 (1963).

(12) See ref. 3.

(13) H. Melchior and W.T. Lynch, I.E.E.E. Trans. Electron. Dev., ED-13, 8 (1966).

(14) Part Two of Annual Report on C.V.D. Contract No. CP3632-66 (August 1966 to December 1967).

FIGURE 1

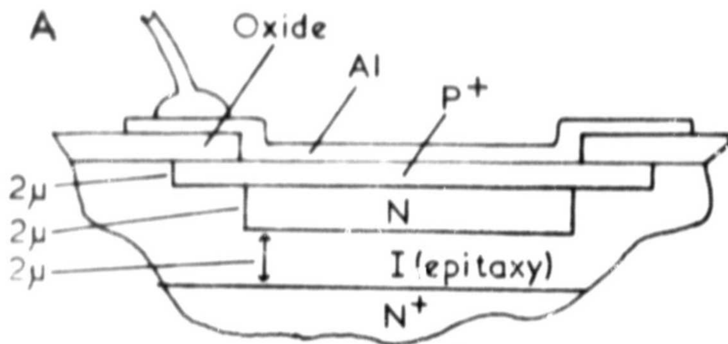

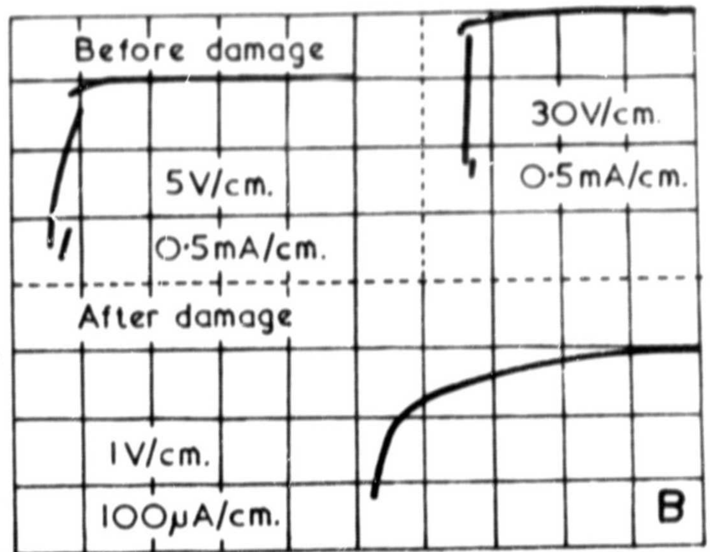

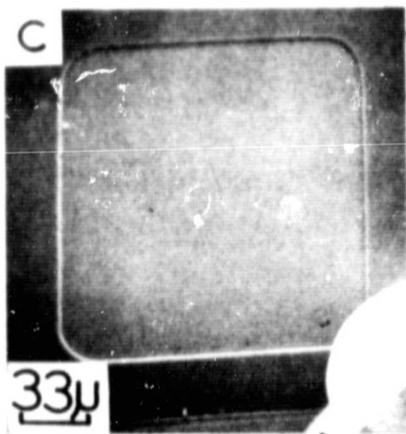

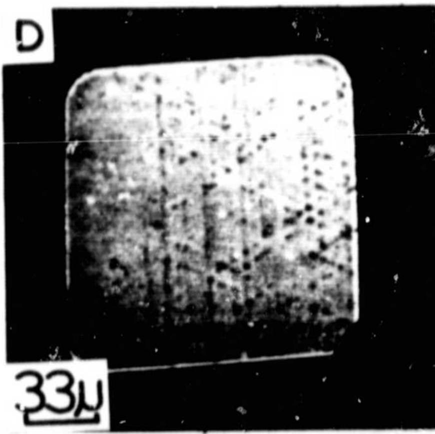

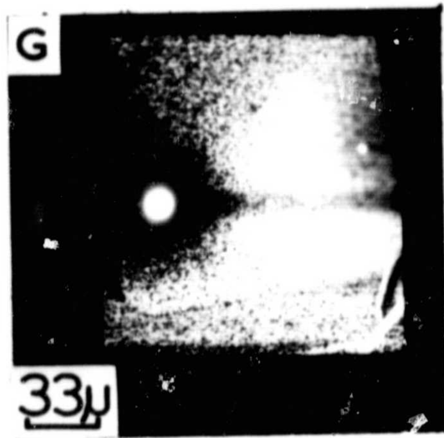

FIGURE 1 Cont.

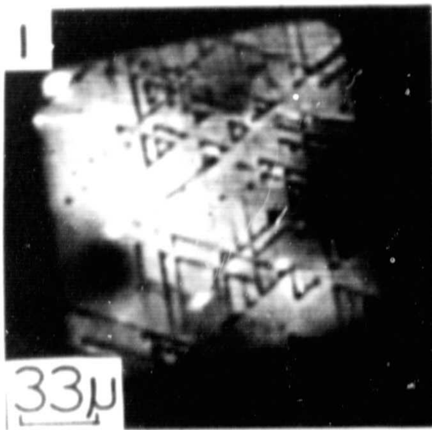

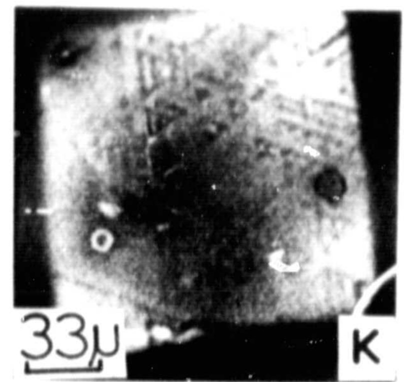

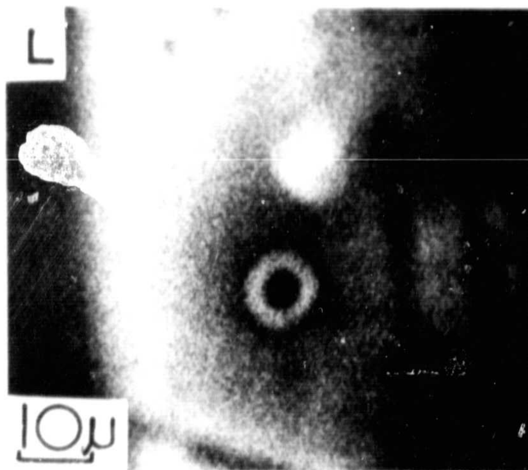

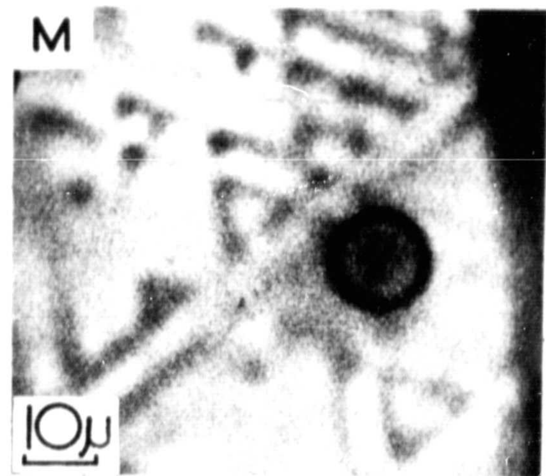

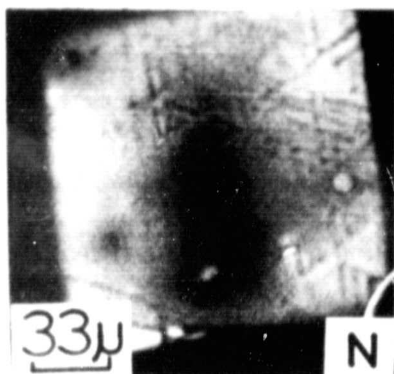

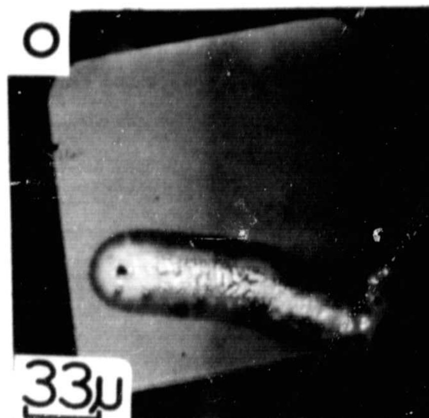

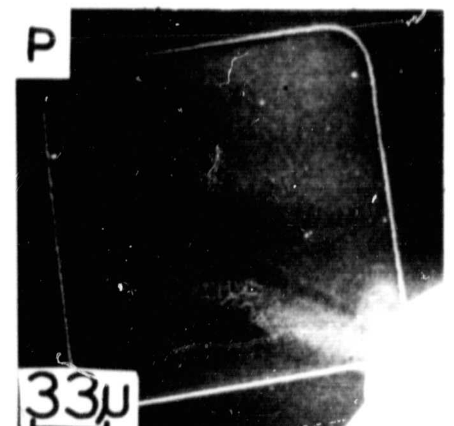

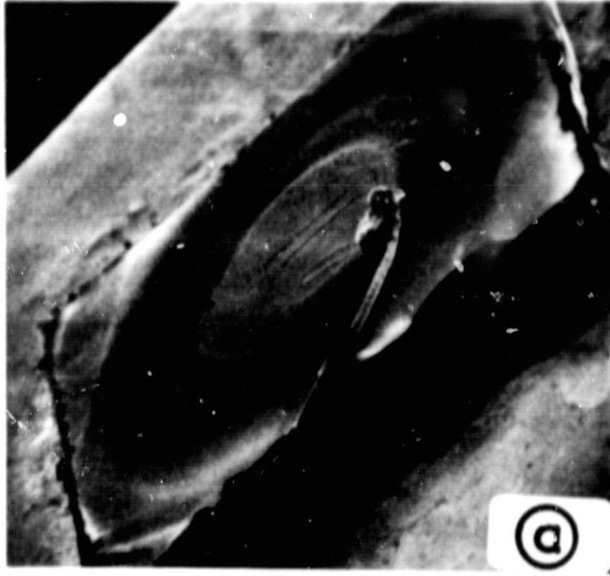

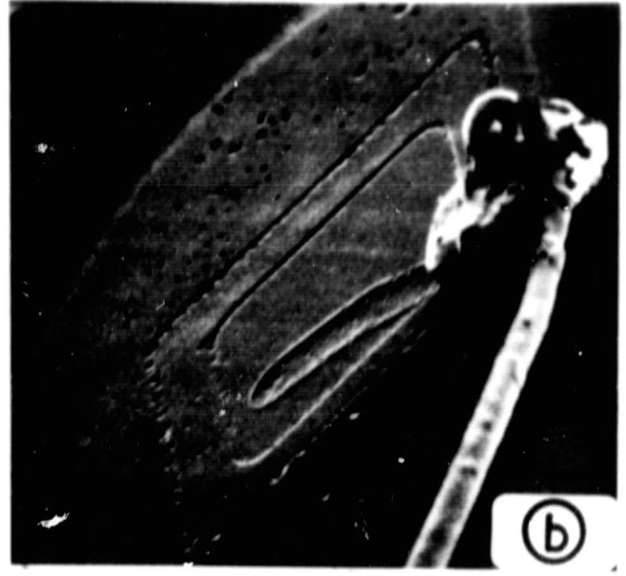

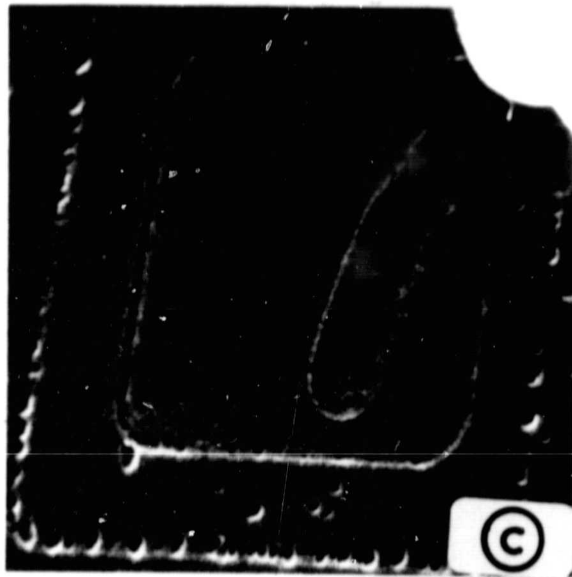

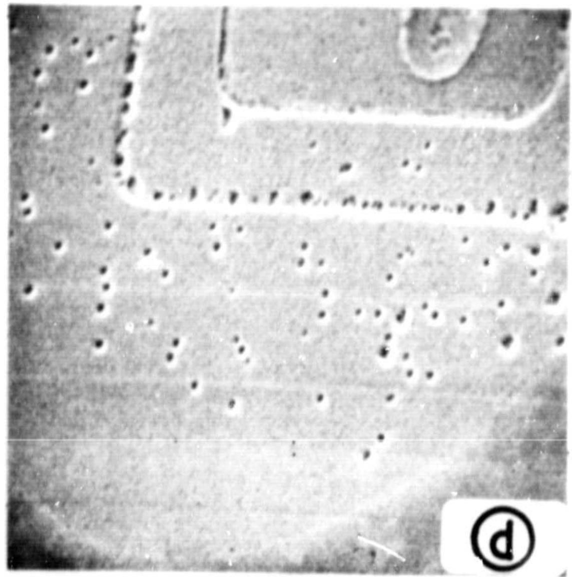

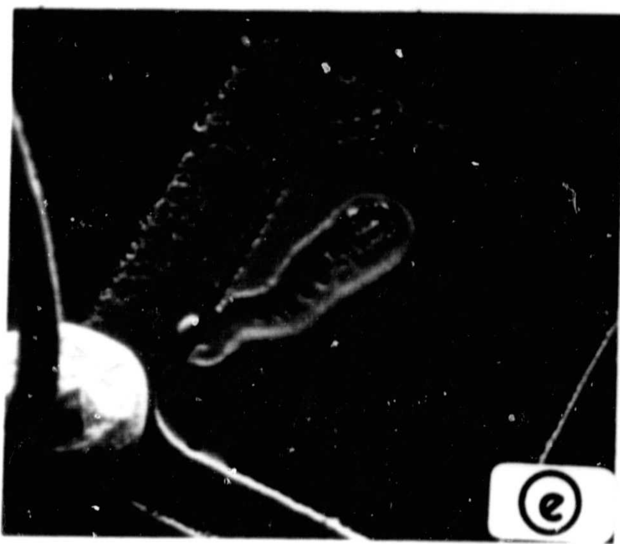

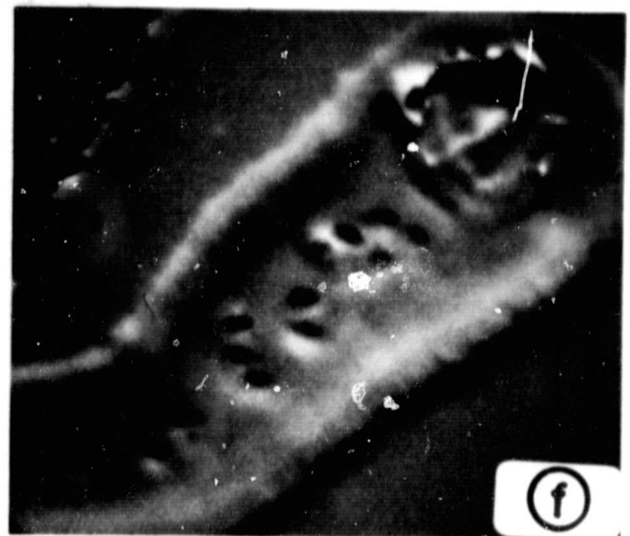

FIGURE.2.

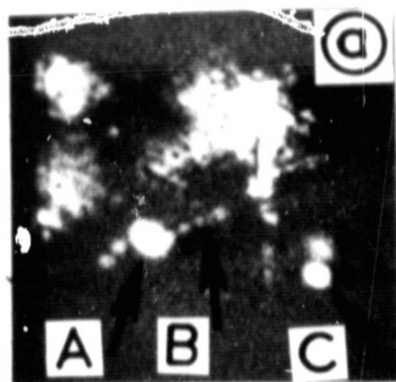

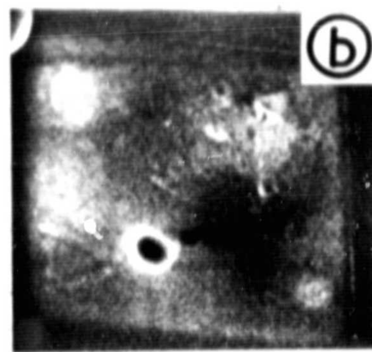

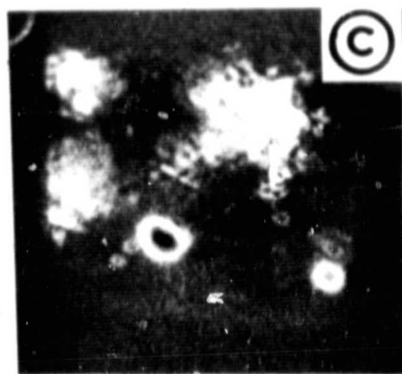

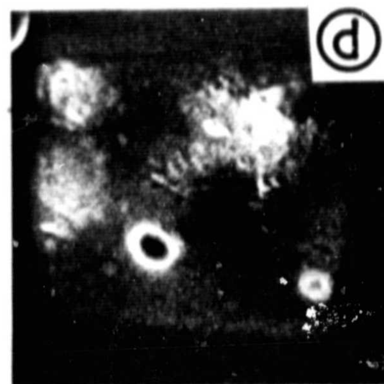

FIGURE. 3.

115·2V, 1·3ma
15 KV BEAM

[A] $< 10^{-12}$ AMP
[B] $\sim 10^{-11}$
[C] $\sim 2 \times 10^{-10}$
[D] $\sim 2 \times 10^{-9}$

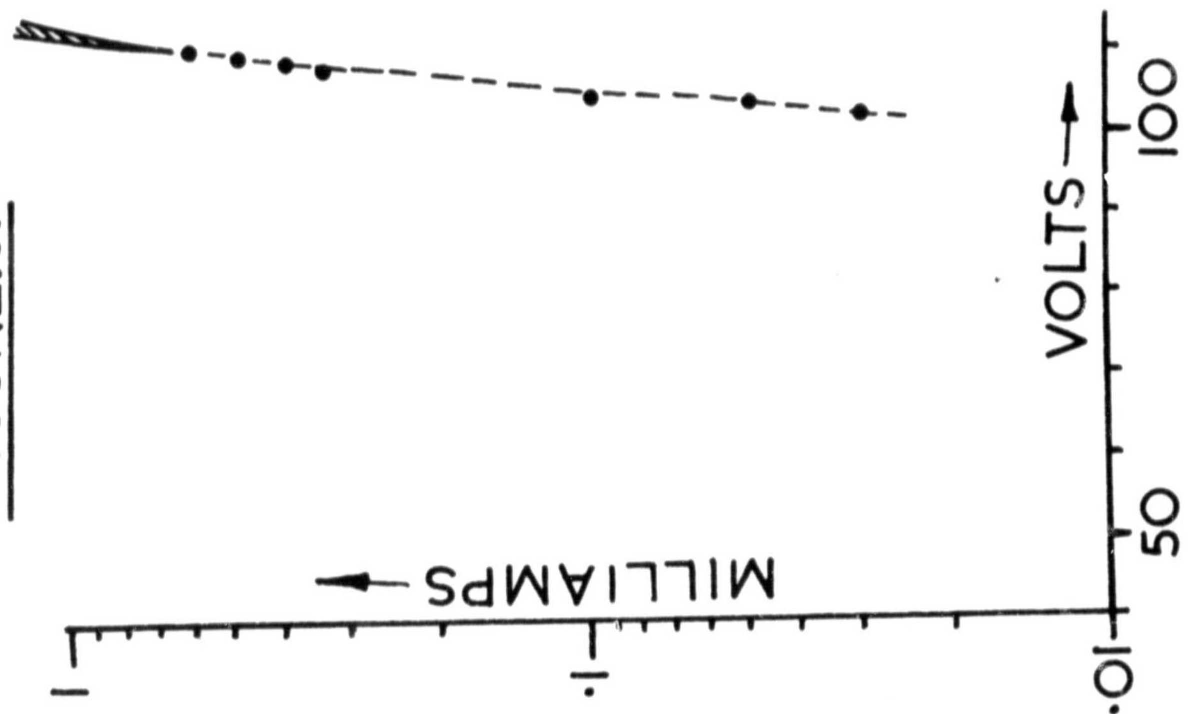

FIGURE. 6.

FIGURE.4.

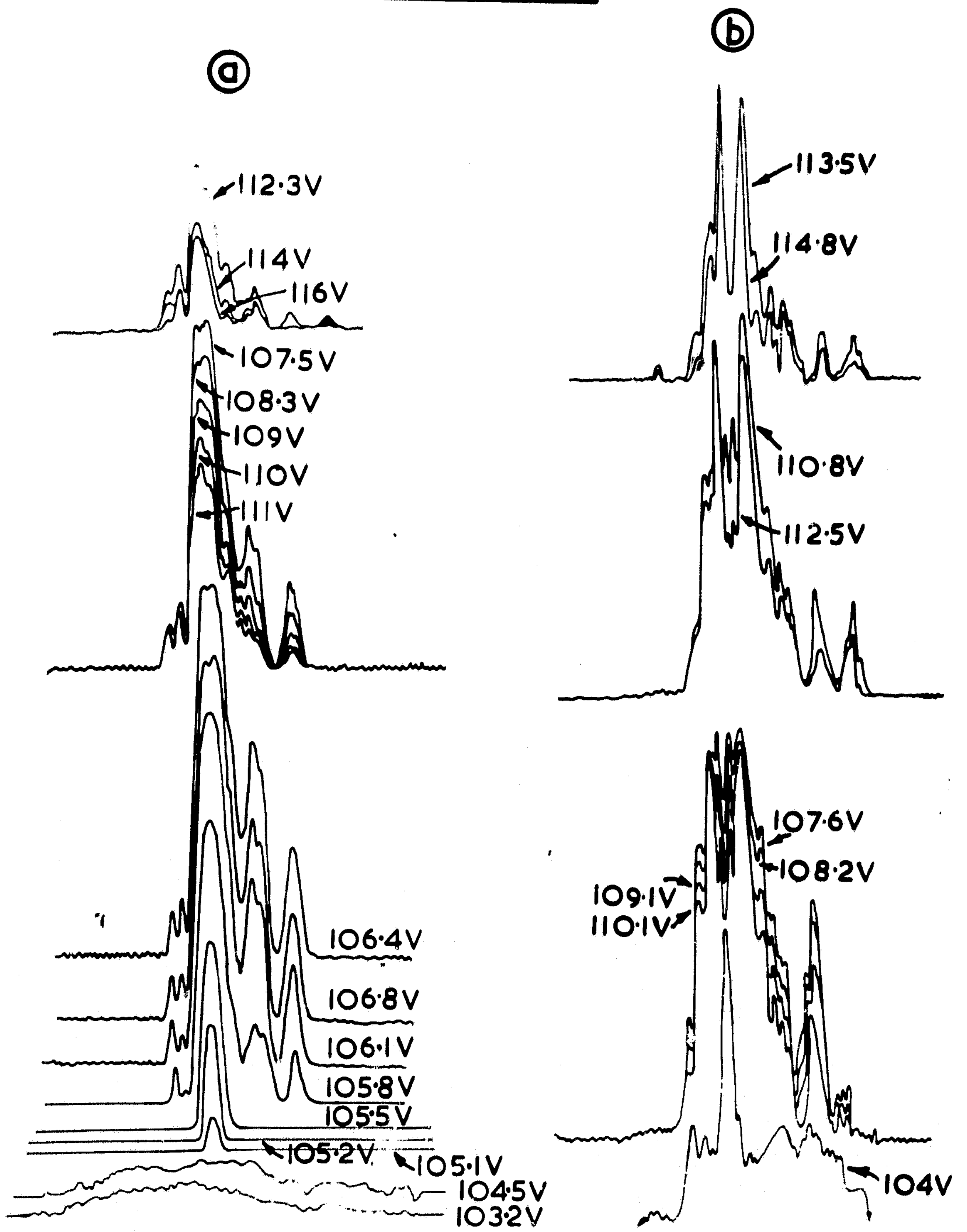

FIGURE.5.

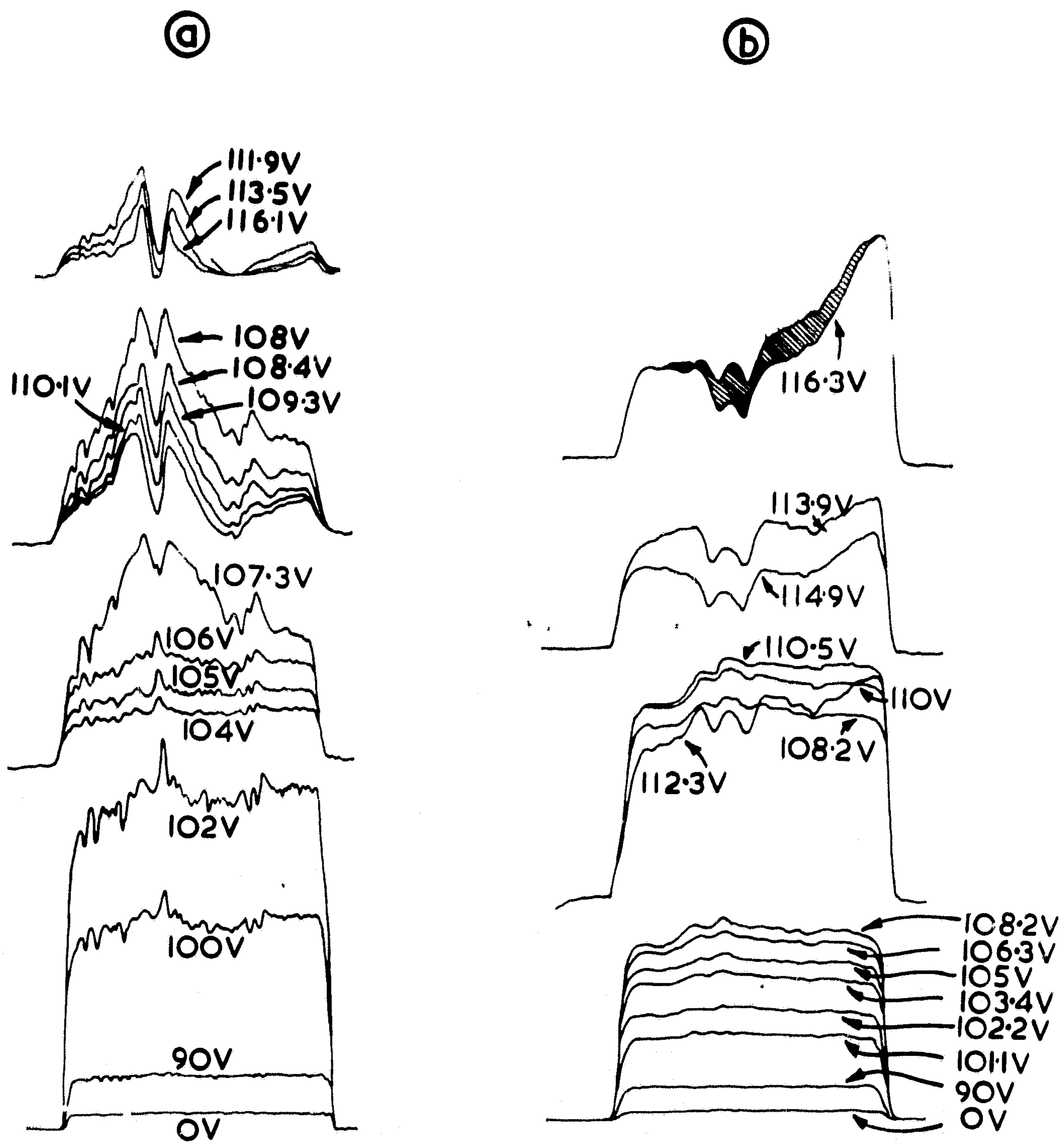

FIGURE. 7.

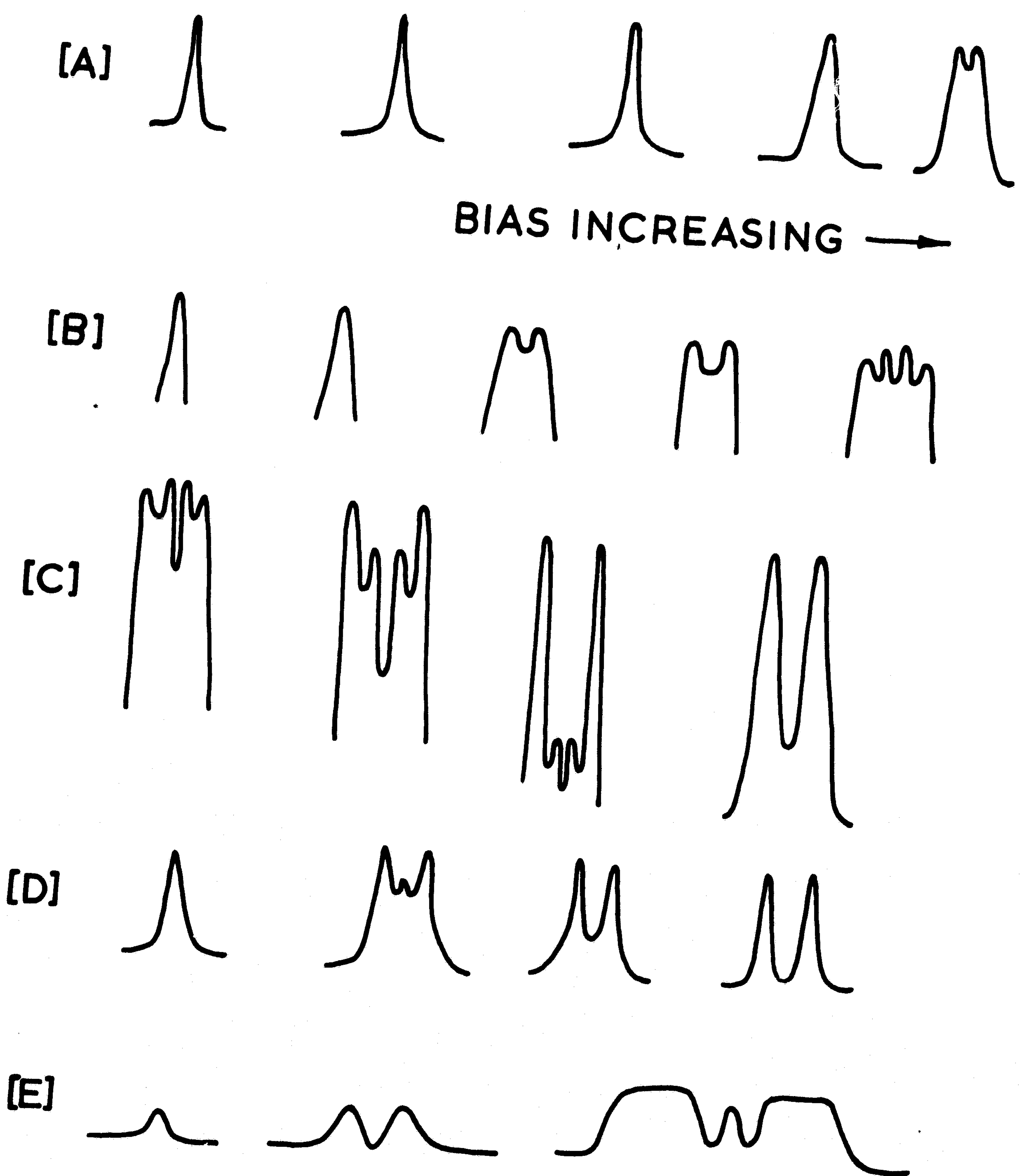

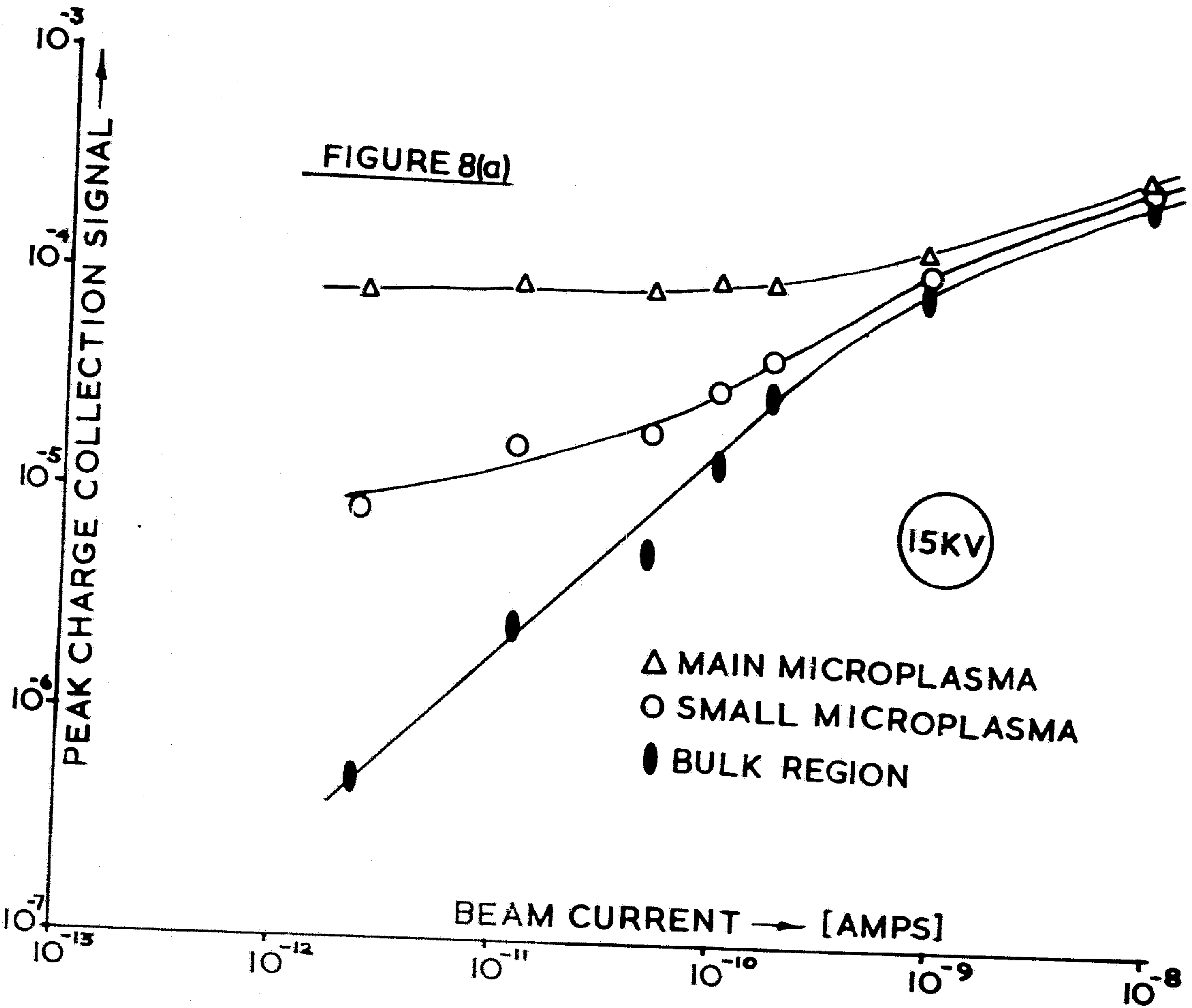
FIGURE 8(a)
PEAK CHARGE COLLECTION SIGNAL
10^{-3}
10^{-4}
10^{-5}
10^{-6}
10^{-7}
15KV
Δ MAIN MICROPLASMA
O SMALL MICROPLASMA
BULK REGION
BEAM CURRENT → [AMPS]
10^{-13}
10^{-12}
10^{-11}
10^{-10}
10^{-9}
10^{-8}

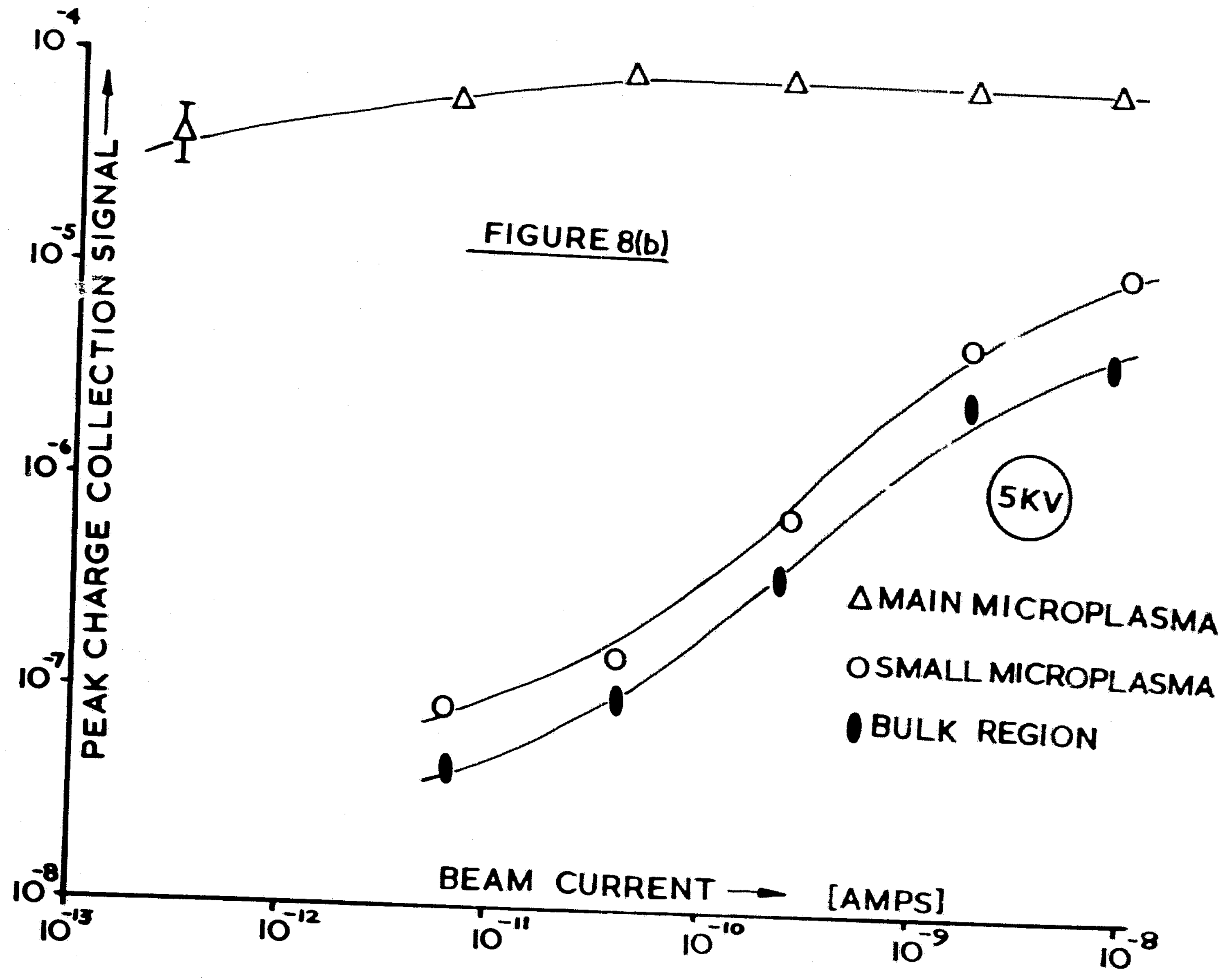

FIGURE 8(b)

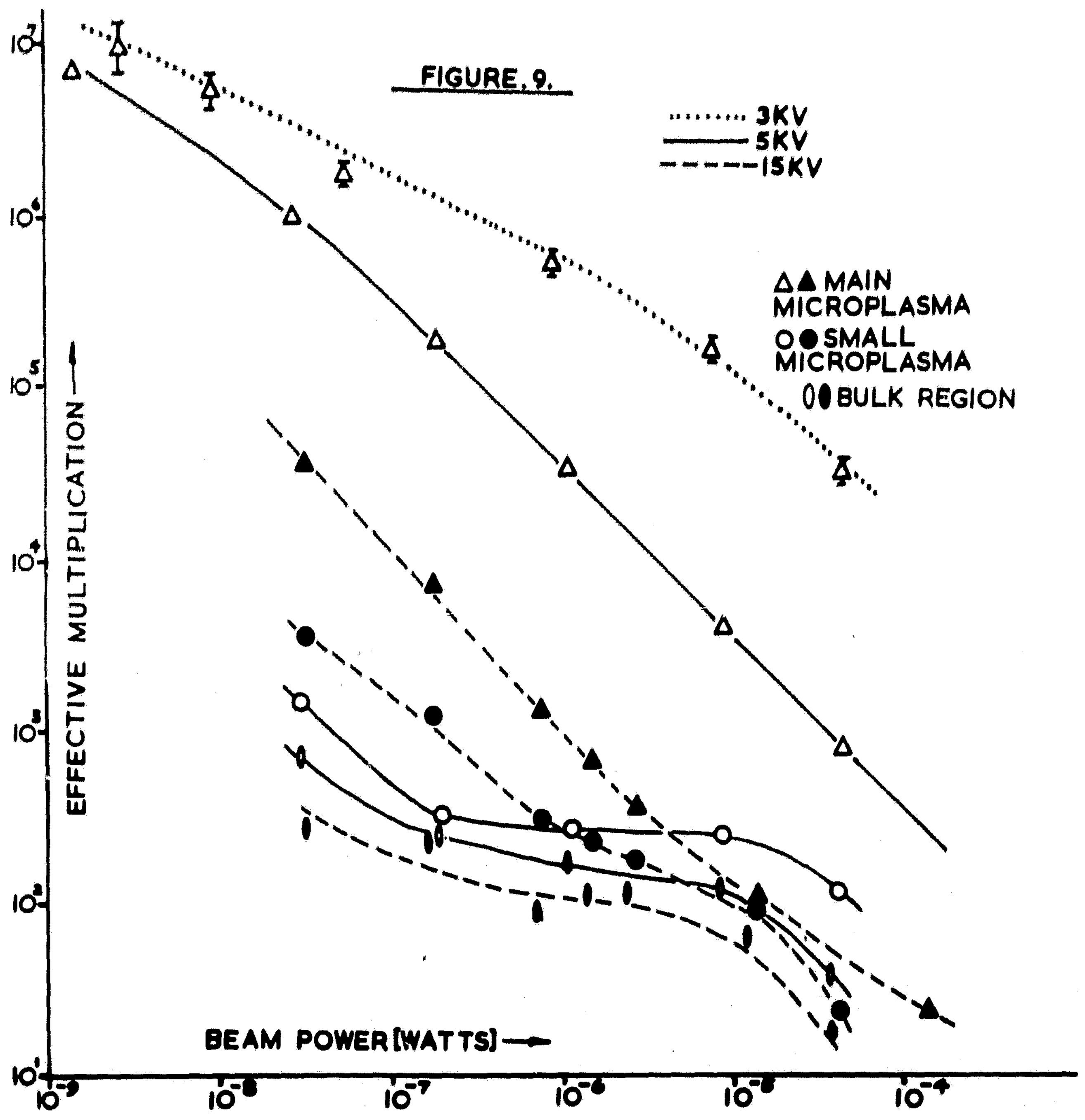
FIGURE. 9.
3KV
5KV
15KV
MAIN MICROPLASMA
SMALL MICROPLASMA
BULK REGION
EFFECTIVE MULTIPLICATION
BEAM POWER (WATTS)
10^7
10^6
10^5
10^4
10^3
10^2
10^1
10^{-9}
10^{-8}
10^{-7}
10^{-6}
10^{-5}
10^{-4}

FIGURE.10.

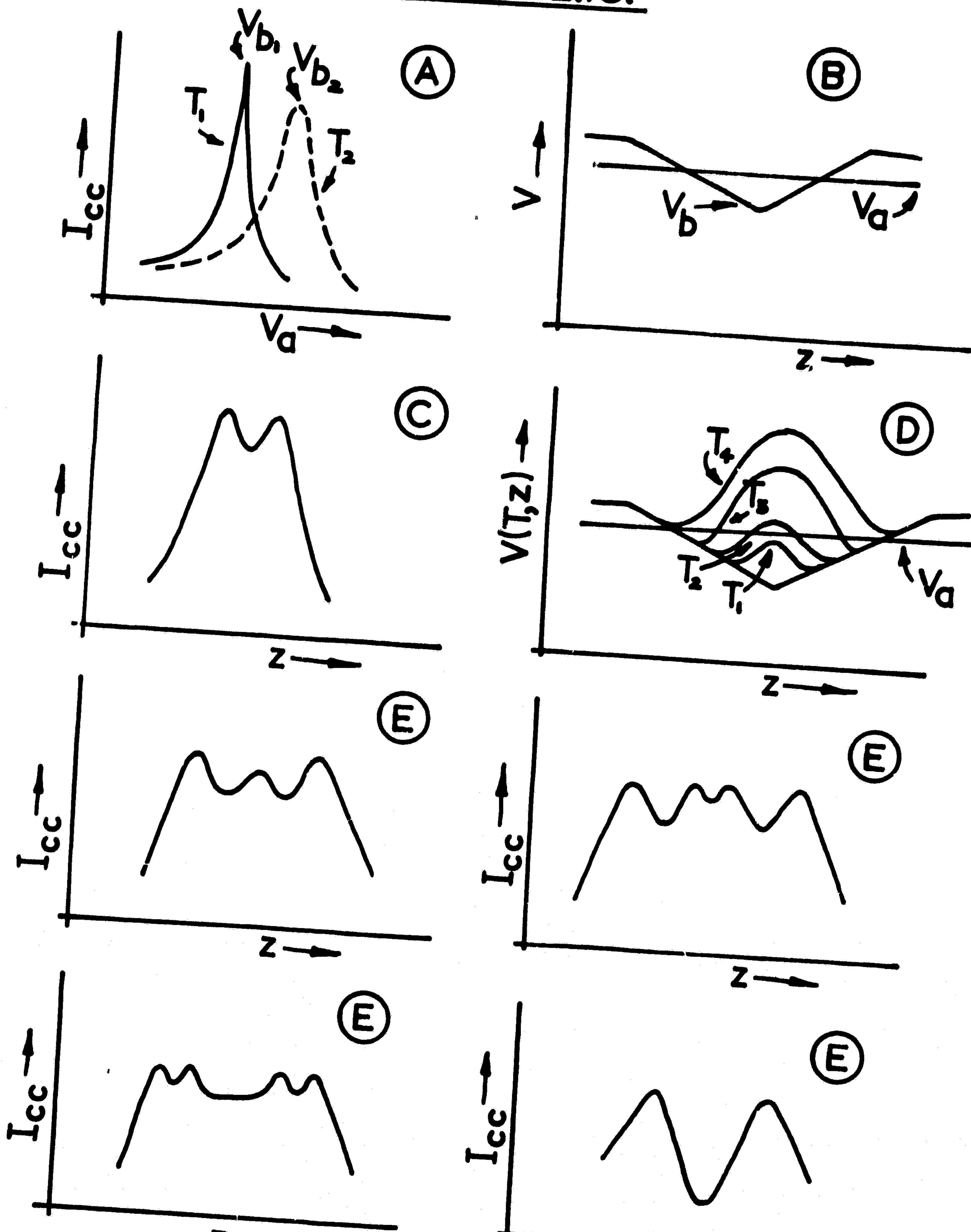

FIGURE.10.